Available online at www.sciencedirect.com

SCIENCE DIRECT®

Applied Clay Science 28 (2005) 297–308

Applied CLAY Science

www.elsevier.com/locate/clay

Mineralogical and physical characterization of the bricks used in the construction of the "Triangul Bastion", Riga (Latvia)

Giuseppe Cultrone[a,*], Inese Sidraba[b], Eduardo Sebastián[a]

[a]*Department of Mineralogy and Petrology, University of Granada, Spain*
[b]*Centre for Conservation and Restoration of Stone Materials, Riga Technical University, Latvia*

Received 10 October 2003; received in revised form 15 November 2003; accepted 2 February 2004
Available online 14 July 2004

Abstract

Bricks proceeding from one of the bastions of the Riga medieval defence wall were studied. Two main type of bricks were identified: one rich in quartz and red coloured and the other with a calcium silicate phase and yellow coloured. The survey of the bastion reveals a partial deterioration of the bricks. It was observed that differences in mineralogy and texture of calcareous and non-calcareous bricks were correlated with their behaviour in hydric and weathering tests. Data from powder X-ray diffraction (presence of high-temperature mineral phase in yellow bricks), optical microscopy (vitrification in yellow bricks), Field Emission Scanning Electron Microscope (development of secondary bubbles due to extensive melting in yellow bricks) and ultrasounds measurements (lower velocity in red bricks) allow to deduce that yellow bricks were fired at a higher temperature than the red ones. The study of the pore system revealed a bad interconnection among pores in yellow bricks (hydric data) since melt isolated the pores and filled the smallest, whereas large pores increased in size (porosimetric data). As a consequence, considering the climatic conditions of the region, yellow bricks are the materials most subjected to environmental alteration. It is in agreement with the freeze–thaw test results. Finally, low contamination of the bricks with water-soluble salts in situ leads to exclude salt-caused decay process. The relevance of these results in the conservation of Cultural Heritage is discussed.

Keywords: Solid bricks; Triangul Bastion Riga (Latvia); Colour of bricks; Mineralogy; Physical characterization; Decay and conservation

1. Introduction

In the 16th century, due to the use of firearms, the old fortification constructions of Riga (Latvia) lost their importance and a new type of defence system, earth ramparts, was developed. The territory was surrounded by a moat, earth wall and bastions. This made Riga one of the strongest fortresses on the

* Corresponding author. Departamento de Mineralogía y Petrología, Facultad de Ciencias, Universidad de Granada, Avda. Fuentenueva s/n, 18002 Granada, Spain. Tel.: +34 958 243340; fax: +34 958 243368.
E-mail address: cultrone@ugr.es (G. Cultrone).

0169-1317/$ - see front matter © 2004 Elsevier B.V. All rights reserved.
doi:10.1016/j.clay.2004.02.005

eastern shore of the Baltic Sea. The "Triangul Bastion" (Fig. 1) represents a part of Riga's medieval defence wall. It was constructed in 1729 and was 6–7 m high. It stood for 130 years until it was partly demolished and flattened. Recent archaeological excavations have provided evidence for the demolition of the upper 3 m of this defence structure. The fortification was constructed near the Daugava River and consisted of two walls: one outer characterized by a slightly slanted wall (5–7°) and reinforced by 12 contrafforts, and another inner wall similar to the outer wall.

Grey and shell dolomite blocks and solid bricks were used for the construction of the wall. Dolomite has been widely used as a construction material in Latvia and its physical characteristics are known (Kondratjeva and Hodireva, 2000), while the properties of these bricks are unknown.

Latvia is situated in the southwest part of the Eastern European Platform (Reimann et al., 2000) where Quaternary deposits generally cover Devonian sediments. Clay deposits are very common during both Devonian and Quaternary periods (Kursh and Stinkule, 1997) and are currently exploited for brick manufacture. Devonian clays lack in carbonates and are rich in illite and kaolinite (Svinka and Svinka, 1997). The principal deposit is located in Vidzeme region, near the city of Cesis (northeast of Latvia). Quaternary clays are rich in carbonates and show similar amounts of illite and kaolinite of those Devonians (Svinka and Svinka, 1997). A large deposit is located in Zemgale region, close to Jelgava City (middle-south of Latvia). Both areas are easily attainable from Riga.

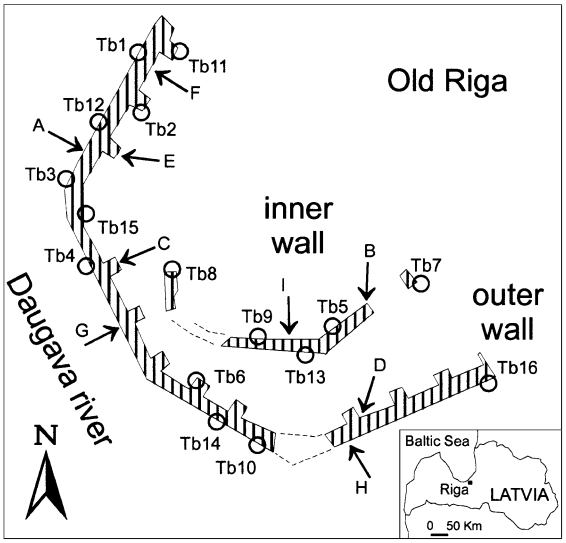

Fig. 1. Plan of the remaining outer and inner walls of the Triangul Bastion, Riga (Latvia). Circles represent sampling location (TB1 to TB7 are yellow bricks; TB8 to TB16 are red bricks); arrows indicate the sampling place for in situ moisture and salt contents determination (A to D are yellow bricks; E to I are red bricks).

Regarding the visual aspect, two main populations of bricks in the walls of "Triangul Bastion" can be distinguished: yellow and red. The abundance of yellow bricks is about 30% in comparison to those red. They have a large variety of dimensions and, probably, different compositions and textures, since according to the building traditions of that time, the bricks to erect the bastion were taken from the construction wastes left from the demolition of buildings. This suggests that the bricks of the bastion differ in their mineralogical and physical characteristics. Furthermore, compared to dolomite blocks, which can attain a high mechanical resistance (about 90 MPa; Kondratjeva and Hodireva, 2000), bricks represent the weakest point of the structure due to a strong anisotropy, typical of these construction materials, which can reduce their resistance to stresses (Binda and Baronio, 1984; Cultrone et al., 2001a).

An examination of the excavated bastion reveals an acceptable preservation of these archaeological remains except for a partial deterioration of some bricks, and in a few cases, their disintegration into powder.

The aim of this work is to characterize the bricks used in the construction of the Triangul Bastion from a mineralogical and textural point of view, to examine their technical behaviour, to deduce the source of the raw materials for possible replacement of altered bricks with new ones, and to establish how the environmental conditions of the region can affect their durability. This investigation is important not only to safeguard a monument of great importance in Latvian Cultural Heritage, but also for the implications these results may have for other similar cases.

Finally, it is important to take into account the climatic condition of Riga. The town has a moderate oceanic climate with a considerable amount of precipitation (516 mm/year). There are remarkable changes in temperature during the year: the maximum is reached in summer (June to August, +30 °C), while the minimum falls in winter (December to February, −27

°C). The annual average temperature is +8 °C. Freeze–thaw cycles are very frequent: they are estimated as about 70 per year. The dominant winds blow from the Baltic Sea and Atlantic Ocean, promoting humid conditions throughout the year (unpublished data from the Meteorological Station of Latvia University).

2. Materials and methods

In order to produce as little damage as possible to the monument, only 16 fragments or fallen bricks, 7 yellow (TB1–TB7) and 9 reds (TB8–TB16), were withdrawn from the structure (Fig. 1).

The mineralogy of the bricks was determined by powder X-ray diffraction (PXRD), using a Philips PW 1710 diffractometer equipped with an automatic slit window. The settings were: CuKα (λ=1.5405 Å), 3–60° 2θ explored area and goniometer speed of 0.05° 2θ/s. Interpretation of mineral phases was performed according to the method proposed by Martín Ramos (1990). Semi-quantitative analysis of minerals was determined using experimentally determined reflectance power of each phase, according to the methods proposed by Culliti (1956) and Rodríguez Gallego et al. (1968).

Texture, mineralogy, the type and size of temper, the vitrification level and the shape of pores were studied by means of optical microscopy (OM; polarized microscope Olimpus DX-50) and Field Emission Scanning Electron Microscope (FESEM; LEO GEMINI 1530) coupled with INCA-200 Oxford microanalysis. Modal analyses from points counted on thin sections were determined by OM. Three hundred points were counted per thin section. FESEM back-scattered electron images (BSE) were acquired using polished thin sections (carbon-coated).

The parameters associated with fluid transport inside the pores were determined by hydric tests. The samples used in these tests were cubic (4 cm per side). Water absorption (NORMAL 7/81, 1981) and evaporation tests (NORMAL 29/88, 1988) were determined by weighing the samples (three samples per brick type) at regular intervals. Forced water absorption was performed according to the methodology described in EN 772-7 (1998). Drying index, apparent and real density, open porosity and degree of connection of pores were calculated.

The distribution of pore access size, the pore volume and the surface area were determined by mercury intrusion porosimetry (MIP), using a Micromeritics Autopore, model 9410, which can generate a pressure of 414 MPa, covering the pore diameter range from approximately 0.03 to 360 μm.

To evaluate the elastic-mechanical characteristic of the bricks, ultrasound propagation velocity (V_P) was measured in the three perpendicular directions using a Steinkamp BP-5 with a pulse frequency of 100 kHz. V_{P1} represents the ultrasound propagation velocity perpendicular to the brick face, V_{P2} is the velocity perpendicular to the end and V_{P3} is perpendicular to the side. From these values, the structural anisotropy (ΔM) was calculated according to the following formula (Guydader and Denis, 1986):

$$\Delta M = \left(1 - \frac{2V_{P1}}{V_{P2} + V_{P3}}\right) \times 100$$

Finally, to individualize the cause of brick decay, the moisture and salt content were measured in situ (nine measurements, four for yellow bricks and five for red bricks; Fig. 1) and the freeze–thaw test carried out on collected samples to determine whether the close to zero thermal oscillation (considering the climate of the region) or the crystallization of salts (proceeding from the ground) or a combination of both phenomena are responsible for the alteration. Soluble salt content measurements were made by wet chemical analyses on water extractions of powder samples: CaO and MgO by complexonometric titration, Na_2O and K_2O by flame photometry, Cl^- by argenometric titration, SO_4^{2-} by sedimentation and NO_3^- by colourimetry. Determination of moisture content in bricks was performed according to EN ISO 12570 (2000). Sampling was done by core drilling at a depth of 22 cm. For the accelerated decay test, 30 cycles of 24 h duration were performed following GOST 7025-91 (1991). These cycles consisted of freezing the samples in air for at least 4 h at −20 °C and thawing in water at +20 °C.

3. Results and discussions

Yellow and red bricks are mineralogically different: the former are characterized by quartz, diopside and minor amounts of feldspar; the latter are much richer in quartz, feldspar and hematite are the other components (Table 1 and Fig. 2). This different mineralogy reflects the use of at least two raw materials during manufacture of the bricks, which could proceed from Jelgava and Cesis, respectively. The presence of diopside in the yellow group suggests the presence of carbonates (maybe dolomite) in the clayey material which react with quartz at high temperatures (González García et al., 1990; Peters and Iberg, 1978) to form $CaMgSi_2O_6$. This suggests that these bricks were fired at a temperature of around 900 °C (Jordán et al., 2001; Cultrone et al., 2001b; Letsch and Noll, 1983).

Moreover, diopside can explain the yellowish colour of the bricks, since carbonates inhibit the growth of iron oxides (Singer and Singer, 1963, Maniatis et al., 1981) favouring the development of lighter colours in ceramic bodies (Klaarenbeek, 1961; Kreimeyer, 1987). The other group lacks carbonates and has a hematite content of more than 5% providing the red pigment of the bricks. The high quartz content, representing 80% of the total mineral phases found in these samples, should be noted. The existence of an amorphous phase (i.e., vitreous phase) is evidenced by a rise of the background noise in the PXRD pattern in the yellow samples (Fig. 2).

Texturally, red bricks are more birefringent with respect to yellow, suggesting different levels of vitrification in the two groups. Red bricks were probably fired at lower temperature. The temper consists or subrounded to angular quartz fragments in both groups (Fig. 3a and b) but the quantity and the dimensions of these crystals are different: they are more abundant in red bricks and the grain size is up to 500 μm and less than 60 μm in the yellow group, confirming that the raw materials used for the manufacturing of the two types of bricks came from different areas. Modal analysis reveals that quartz concentration is higher in red bricks (45%) with respect to yellow (30%). These values are significantly lower compared to PXRD analysis (Table 1). These differences can be explained with the difficulty of OM to distinguish crystals of a few micrometers' size. For this reason, it was impossible to count phases as diopside, hematite and feldspar. On the other hand, PXRD technique is not able to determine vitreous phase concentrations which can be remarkable for yellow bricks. Modal analysis showed

Table 1
Results of powder X-ray diffraction analyses of the two types of bricks

	Qtz	Fs	Hem	Di
TB1	40	15	–	45
TB2	45	20	–	35
TB3	50	20	–	30
TB4	45	15	–	40
TB5	55	10	–	35
TB6	40	10	–	50
TB7	40	15	–	45
$\bar{X}_{Yellow}$	45	15	–	40
σ_{Yellow}	5.77	4.08	–	7.07
TB8	80	10	10	–
TB9	75	20	5	–
TB10	80	10	10	–
TB11	70	20	10	–
TB12	85	10	5	–
TB13	85	10	5	–
TB14	80	10	10	–
TB15	85	10	5	–
TB16	80	10	10	–
$\bar{X}_{Red}$	80	12	8	–
σ_{Red}	5.00	4.41	2.64	–

Qtz=quartz; Fs=feldspar; Hem=hematite; Di=diopside. Mineral symbols after Kretz (1983); $\bar{X}$=mean values; σ=standard deviation.

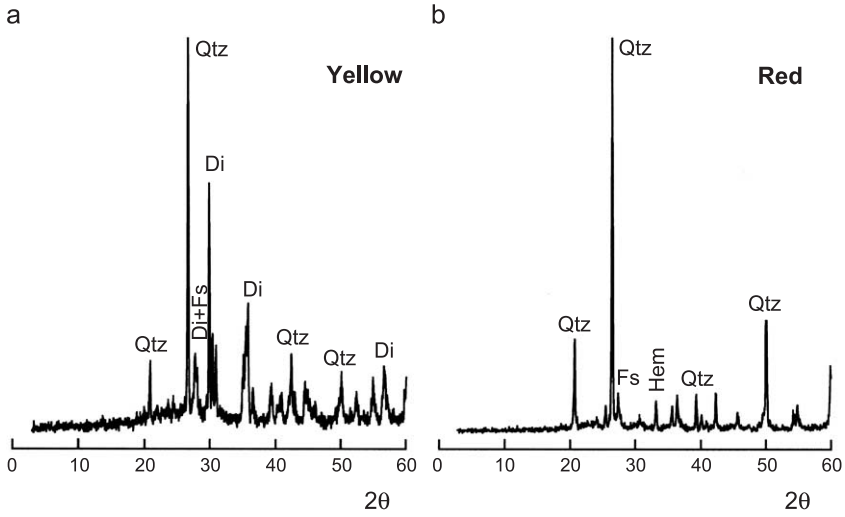

Fig. 2. Yellow (a) and red (b) bricks powder X-ray diffraction patterns. Legend (mineral symbols after Kretz, 1983): Qtz=quartz; Fs=feldspar; Hem=hematite; Di=diopside. CuKα X-ray radiation, λ=1.5405 Å.

that the matrix prevail in this group (70%) with respect to red bricks (55%). The matrix has different appearances due to the development of hematite in red bricks where it can recognized as few small crystal dispersed in a uniform red Fe-rich surface (Fig. 3d), while the matrix is lighter in yellow bricks (Fig. 3c). Macropores have no preferential orientation, show irregular shape and seem to be more abundant in yellow bricks (30% according to modal analysis) than in red (20%, Fig. 3e and f). Finally, black stains proceeding from burnt organic matter present in the raw material can be recognized (Fig. 3f).

BSE images give an interesting picture on the different texture and mineralogy developed by two brick groups. Yellow bricks (Fig. 4a) show a secondary bubbles formation due to the extensive melting of clay particles in the matrix. Pores are ellipsoid with smooth edges and coalesce resulting in the so-called "cellular structure" (Tite and Maniatis, 1975). Interconnectivity among particles is extensive. In red bricks, pores show

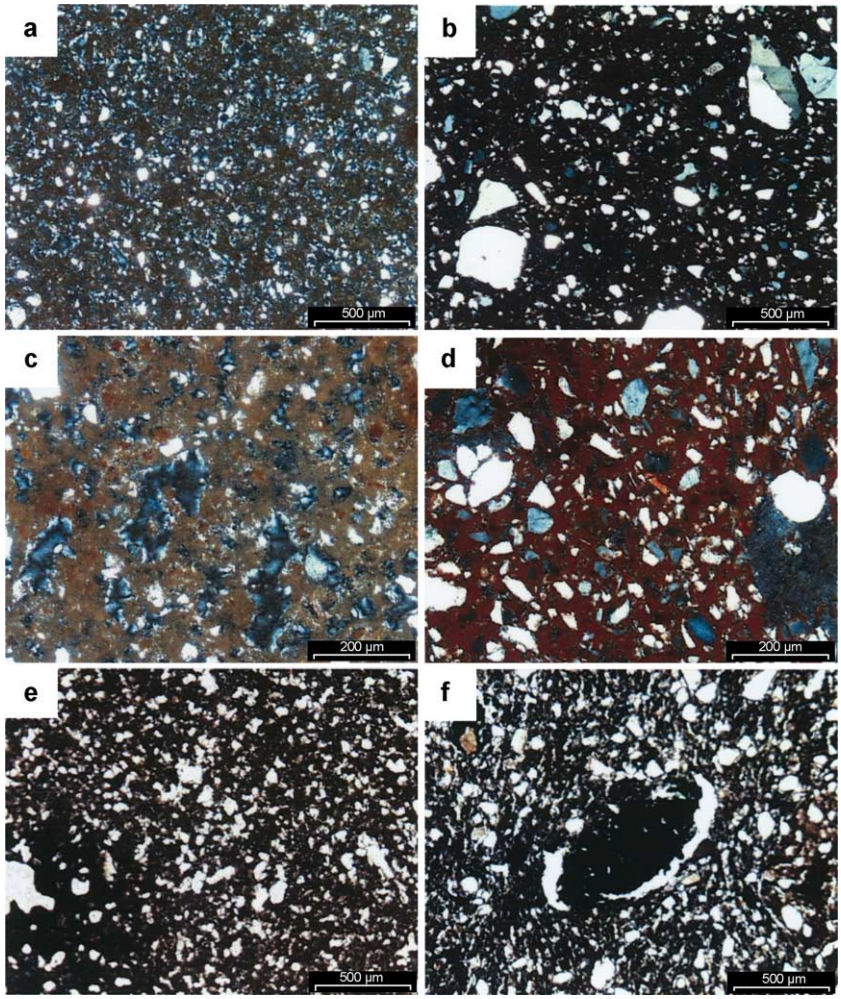

Fig. 3. Optical microscopy photographs: yellow bricks to the left and red bricks to the right. General aspect of yellow bricks (a) and red bricks (b) with a larger amount of quartz crystals in the latter; detail of yellow (c) and red bricks (d). The colour of the matrix is clearly different due to the presence of hematite in red bricks; appearance of the porosity in both groups. Yellow bricks show lower porosity (e) with respect to red bricks (f) in which a black stain, due to the firing of organic matter, can be seen in the centre of the image. (For the interpretation of the references to colour in this figure legend, the reader is referred to the web version of this article.)

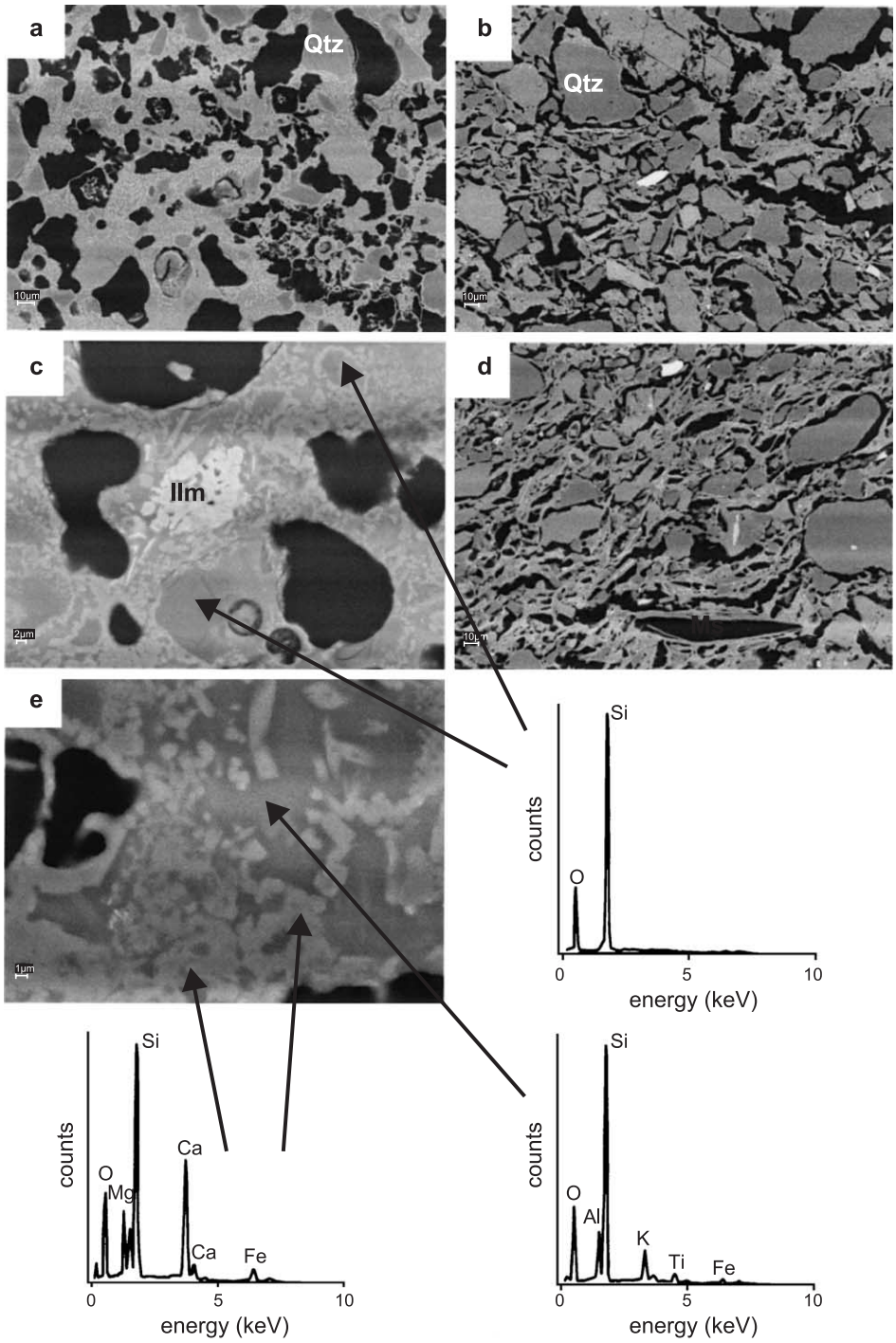

Fig. 4. BSE images and EDX analyses of brick samples: (a) general aspect of yellow bricks showing ellipsoid pores; (b) texture of red bricks in which pores present irregular shapes; (c) detail of yellow brick in which quartz fragments are surrounded by bright rims; (d) partial orientation of elongated pores in red bricks and exfoliation of phyllosilicates along their basal planes; (e) detail of prismatic diopside crystals scattered in the matrix (see EDX analyses). Legend: Qtz=quartz; Ilm=ilmenite; Phy=phyllosilicate.

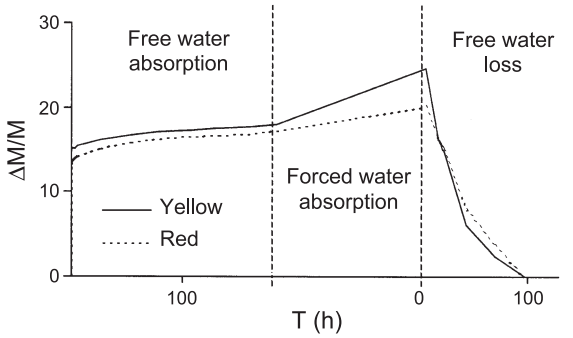

Fig. 5. Free absorption, forced absorption and drying of yellow and red bricks over time (in hours).

an angular shape, are scattered and are more evenly distributed compared to yellow bricks, but the union among particles is limited (Fig. 4b) indicating of a low vitrification level. Some preferred orientation of elongated pores is detected most probably associated to the layering of phyllosilicates. These crystals (Phy in Fig. 4d) show marked exfoliation along their basal planes following the loss of K^+ and OH^- groups (Rodríguez Navarro et al., 2003). Detailed images of yellow bricks permit to recognize a few micrometers of light-isolated crystals with a prismatic habit, or in some cases, as rims surrounding quartz crystals (Fig. 4c and e). Their composition correspond to a calcium magnesium silicate phase (i.e., diopside in EDX results). EDX analysis of the matrix shows Al and K together with Si, proceeding after clay particles breakdown.

Regarding hydric behaviour, Fig. 5 shows how yellow bricks absorb water faster than red bricks. When samples are subjected to forced absorption, it is evident that yellow bricks absorb more water. This depends on the porous system, which is not the same in the two groups. In order to evaluate the pore interconnection (Ax, Table 2), free and force absorption were compared following the equation (Cultrone et al., 2004):

$$\mathrm{Ax} = \frac{\mathrm{Af} - \mathrm{Al}}{\mathrm{Af}} \times 100,$$

where Al is the free water absorption and Af is the forced water absorption.

As the difference between Al and Af increases, the interconnectivity among the pores diminishes, suggesting the existence of pores of difficult access that

Table 2
Hydric and porosimetric parameters (labelled with the suffix MIP) of two types of bricks

	Al	Af	Ax	ID	ρ_A	ρ_R	Pa	$Pt_{(MIP)}$	$S_{(MIP)}$
TB1	17.86	24.72	27.75	0.11	1.23	1.77	33.27	37.02	1.91
TB2	16.96	23.16	26.77	0.25	2.08	4.64	34.27	34.28	1.79
TB3	18.37	25.16	26.99	0.08	2.04	4.21	32.67	33.80	1.87
TB4	16.39	22.87	28.33	0.04	1.97	3.93	38.50	37.41	1.78
TB5	17.51	24.07	27.25	0.12	2.51	3.44	37.57	34.20	1.85
TB6	20.89	29.04	28.06	0.11	2.09	4.89	33.93	34.81	2.13
TB7	17.40	23.56	26.15	0.16	1.80	3.88	35.26	35.31	1.86
$\bar{X}_{Yellow}$	17.91	24.65	27.33	0.12	1.96	3.82	35.07	35.26	1.88
σ_{Yellow}	1.46	2.10	0.77	0.07	0.39	1.03	2.20	1.42	0.12
TB8	17.55	19.92	11.90	0.15	2.08	3.54	38.30	34.11	5.01
TB9	18.57	20.72	10.38	0.11	1.91	3.16	36.95	37.10	4.45
TB10	17.23	19.54	11.82	0.16	2.09	3.53	35.15	31.08	4.02
TB11	18.98	23.17	18.08	0.11	2.23	3.88	35.88	36.03	3.64
TB12	15.16	18.66	18.76	0.23	2.02	3.64	38.46	33.22	4.13
TB13	15.68	19.23	18.46	0.06	1.98	3.02	38.21	34.77	3.24
TB14	18.07	20.13	10.23	0.09	2.09	3.61	39.48	32.13	4.17
TB15	18.34	20.36	9.92	0.10	2.14	3.80	41.08	35.70	5.20
TB16	15.22	18.61	18.22	0.12	2.13	3.70	35.82	32.05	4.25
$\bar{X}_{Red}$	17.20	20.04	14.20	0.13	2.07	3.54	37.70	34.02	4.23
σ_{Red}	1.48	1.38	4.03	0.05	0.09	0.28	1.93	2.05	0.61

Al=free absorption (%); Af=forced absorption (%); Ax=degree of pore interconnection (%); ID=drying index; ρ_A=apparent density (g cm^{-3}); ρ_R=real density (g cm^{-3}); Pa=open porosity (%); $Pt_{(MIP)}$ porosity determined by MIP (%); $S_{(MIP)}$=surface area (m^2/g); $\bar{X}$=mean values; σ=standard deviation.

are not accessible under normal conditions (only under vacuum), which indicate, to a certain extent, the development of melt in the bricks. Yellow bricks show a worse pore interconnection (Ax=27.33% against 14.20% in red bricks), a typical tendency in highly vitrified bricks (Cultrone et al., 2004), confirming the observations by OM and FESEM.

The evaporation of water is similar in both groups as shown by the drying curves (Fig. 4) and the drying index (ID, Table 2). Yellow bricks are slightly denser (ρ_R) than red as they are more vitrified and also contain a greater amount of higher-density mineral phases (ρ_{Di}=3.30 g/cm^3 compared to $\rho_{Qtz\alpha}$=2.53 g/cm^3). Finally, the high values of porosity measured in these materials (Pa>32%; Table 2) reflect the presence of the burnt organic matter mentioned above (probably straw or coal powder), frequently used to increase the porosity of the bricks (Esbert et al., 1997).

The small difference in porosity between the two brick groups is confirmed by MIP studies. The porosity ($Pt_{(MIP)}$) is slightly lower in red bricks with a high concentration of pores with radius in the range of 1–10 μm (Fig. 6). As can be seen, in yellow bricks, larger pores (the majority with radius close to 10 μm) predominate since the escape of gases trapped in the samples favours their formation (Freestone and Middleton, 1987; Veniale, 1990), while the smaller pores are filled by melt during vitrification (Delbrouck et al., 1993; Orts et al., 1993). Consequently, the surface area value ($S_{(MIP)}$) is lower in yellow bricks ($S_{(MIP)}$=1.88 m^2/g against 4.23 m^2/g in red bricks). The different porosity explains why the interconnectivity index is lower in yellow bricks as observed with hydric tests (Ax, Table 2).

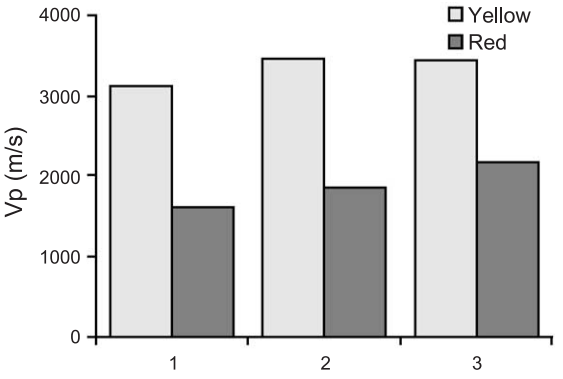

brick	ΔM
Yellow	9.55
Red	20.29

Fig. 7. Histograms of the ultrasound measurements on yellow and red bricks. The *Y* axis shows velocity (in m/s) and the *X* axis the direction of wave propagations (1: is perpendicular to face; 2: is perpendicular to end; 3: is perpendicular to side). A table showing structural anisotropy (Δ*M*) according to Guydader and Denis (1986) is also shown.

Ultrasound measurements show that V_{P2} and V_{P3} values are always higher than V_{P1}. This circumstance is due to the orientation of the clay minerals parallel to the largest face of the brick during manufacturing. Thus, their location perpendicular to the direction of propagation of the ultrasound waves V_{P1}, produces a laminar anisotropic structure in the bricks. V_{P2} and V_{P3}, in turn, can provide variable results depending on

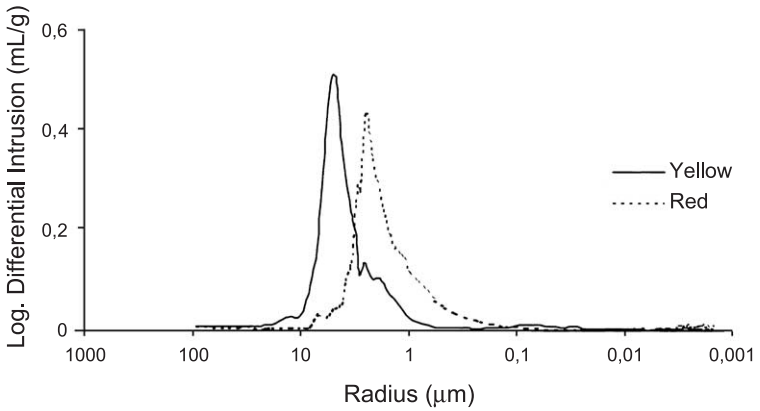

Fig. 6. MIP pore size distribution curves of yellow and red bricks. Log differential intruded volume (ml/g) versus pore radius (μm).

Table 3
Moisture and salt content in bricks of Triangul Bastion ($\bar{X}$=mean values; σ=standard deviation)

	Moisture (mass %)	Salt contamination (mass %)					
	Depth 22 mm	Na_2O	K_2O	Cl^-	SO_4	CaO	MgO
A	15	0.02	0.04	0.02	0.09	0.08	0.00
B	12	0.03	0.04	0.02	0.10	0.11	0.00
C	16	0.00	0.04	0.00	0.07	0.09	0.00
D	16	0.02	0.03	0.02	0.11	0.14	0.00
$\bar{X}_{Yellow}$	14.75	0.02	0.04	0.02	0.09	0.11	0.00
σ_{Yellow}	1.89	0.01	0.01	0.01	0.02	0.03	0.00
E	11	0.02	0.03	0.03	0.02	0.15	0.00
F	14	0.06	0.05	0.04	0.00	0.11	0.00
G	17	0.03	0.06	0.04	0.05	0.13	0.01
H	15	0.01	0.05	0.05	0.06	0.07	0.00
I	16	0.03	0.04	0.04	0.02	0.14	0.00
$\bar{X}_{Red}$	14.60	0.03	0.05	0.04	0.03	0.12	0.00
σ_{Red}	2.30	0.02	0.01	0.01	0.02	0.03	0.00

the orientation of the clay with respect to the side of the mould used to shape the raw material and, therefore, of the planar minerals with respect to the transducers.

From a mechanical point of view, ultrasound confirms the differences between these two types of bricks. The velocity is higher in yellow bricks (>3100 m/s) with respect to red (≤2200 m/s, Fig. 7), revealing a stronger structure due to the extensive vitrification and densification as was observed by OM, FESEM and hydric tests. Furthermore, the structural anisotropy (ΔM) is lower in yellow bricks, which seems logical if we consider that, at high temperatures, the phyllosilicates transform into one or a series of phases plus a glass (Rodríguez Navarro et al., 2003; Brearley and Rubie, 1990) and thus the laminar morphology is lost.

The data from the analyses of salt and moisture contamination show the high content of moisture in masonry (~15%, Table 3), while salt concentration within the bricks are very low or absent and cannot be considered directly responsible for the deterioration of the bastion.

The freeze–thaw test reveals that yellow bricks have low frost resistance compared to red bricks (Fig. 8). In fact, yellow samples break between the 10th and the 18th cycle of this test, while red samples usually reach 30 cycles without breaking. The apparent contrast between these results and the others, specially according to ultrasound data where yellow bricks suggest a better behaviour, can be explained as follows. It is well known that the presence of large pores is considered beneficial to frost resistance of

Fig. 8. Appearance of some red and yellow bricks after freeze–thaw test. Samples that have withstood under accelerated aging test can be distinguished from those totally broken. (For interpretation of the references to colour in this figure legend, the reader is referred to the web version of this article.)

bricks, whereas small pores lead to greater damage (Maage, 1980). However, it is equally important the interaction between the pore structure, their degree of interconnection (Ax), and the weathering (Hansen and Kung, 1988). During the first cycles, the high vitrification of yellow bricks favours a lesser deterioration of the samples. In fact, the weight loss is higher in red bricks (0.3% weight loss) than in yellow (0.1%), but when the water can spread into the badly connected capillaries, a rigid vitrified structure (yellow bricks) breaks, while a non-vitrified more elastic structure (red bricks) better resists the ice crystallization pressure, resulting only in a loss of small fragments without breaking.

4. Conclusions

The detailed study of all the variables involved in the characterization of bricks of "Triangul Bastion", Riga (Latvia) provides objective data that help to determine the technical quality of this type of clay product.

Two groups of bricks (yellow and red coloured, respectively), different in the mineralogy and almost certainly prepared using two types of raw materials, proceeding from Jelgava and Cesis, have been identified. The presence of diopside only in the yellow bricks may be due to the reaction at high temperature of a pre-existing dolomite with quartz (Capel et al., 1985). This silicate phase can be recognized as isolated crystals dispersed into the matrix or as rims surrounding quartz crystals.

Moreover, carbonate favours a lighter colour in bricks as the iron present in the matrix is "trapped" in the calcium silicate structure (Maniatis et al., 1981) and prevents the formation of hematite. In the raw material for the preparation of red bricks, the absence of carbonate facilitates the formation of iron oxides which give the bricks their red pigmentation.

Different raw materials result in bricks with different physical behaviour (Manning, 1995) especially bearing in mind that only yellow bricks are well vitrified, suggesting a different firing temperature for the two groups. The vitreous phase in yellow bricks favours the production of less anisotropic bricks and reduces water penetration (by diminishing the pores interconnection and increasing the pore radius). These conclusions are consistent with hydric, porosimetric and ultrasound data. Regarding brick alteration, the salt crystallization phenomenon is negligible, thus not considered as a decay agent. The principal source of alteration is the damp in masonry deriving from rainwater and the high capillarity from the ground due to the location of the bastion, near the Daugava River, and associated with the cold winter in Riga. It was demonstrated that, due to their pore structure, yellow bricks are more prone to alteration, especially during the winter when physical deterioration due to freeze–thaw alternation occurs.

For future restoration interventions of the bastion, the choice of a correct firing temperature, which cannot be standardized, as it depends on the type of raw material (e.g., with or without carbonates), is a fundamental parameter affecting brick quality (Cultrone et al., 2001a,b). As a general remark, it is possible to manufacture new bricks according to specific needs, varying the composition of the raw material and the firing temperature, but this requires that the characteristics of the historic bricks be previously determined. In fact, when the substitution of highly altered bricks by new ones is necessary, it is advisable not only to take into account aesthetic, textural and compositional approaches, but also similarities in hydric behaviour in order to avoid differential migration of humidity that may damage other areas of the monument. In the case of "Triangul Bastion", taking into account the obtained results, the manufacture of new bricks similar to the red ones is suitable for restoration work.

These results make a notable contribution to future work on the conservation of the numerous monuments constructed partially or totally with bricks, when the more proper type of raw materials must be chosen to produce bricks for replacement.

Acknowledgements

This research has been supported by a Marie Curie Fellowship of the European Community Programme "Energy, Environment and Sustainable Development" under contract number EVK4-CT-2002-50006, by the Research Group RNM179 of

the Junta de Andalucía and by the Research Project DGI-MAT-2000-1457. We thank the Centro de Instrumentación Científica of the Granada University for allowing us to use their FESEM-INCA. We also thank the in-depth review by Prof. M. Setti and an anonymous referee.

References

Binda, L., Baronio, G., 1984. Measurement of the resistance to deterioration of old and new bricks by means of accelerated aging tests. Durability of Building Materials 2, 139–154.

Brearley, A.J., Rubie, D.C., 1990. Effects of H_2O on the disequilibrium breakdown of muscovite+quartz. Journal of Petrology 31, 925–956.

Capel, J., Huertas, F., Linares, J., 1985. High temperature reactions and use of Bronze Age pottery from La Mancha, Central Spain. Mineralogica et Petrographica Acta 29A, 563–575.

Culliti, B.D., 1956. Elements of X-ray Diffraction. Addison-Wesley Publishing, Reading, MA, USA, pp. 378–401. Chap. 14.

Cultrone, G., Sebastian, E., Cazalla, O., Nechar, M., Romero, R., Bagur, M.G., 2001a. Ultrasound and mechanical tests combined with ANOVA to evaluate brick quality. Ceramics International 27, 401–406.

Cultrone, G., Rodriguez Navarro, C., Sebastian, E., Cazalla, O., de la Torre, M.J., 2001b. Carbonate and silicate phase reactions during ceramic firing. European Journal of Mineralogy 13, 621–634.

Cultrone, G., Sebastian, E., Elert, E., de la Torre, M.J., Cazalla, O., Rodríguez Navarro, C., 2004. Influence of mineralogy and firing temperature on the porosity of bricks. Journal of the European Ceramic Society 24, 547–564.

Delbrouck, O., Janssen, J., Ottenburgs, R., Van Oyen, P., Viaene, W., 1993. Evolution of porosity in extruded stoneware as a function of firing temperature. Applied Clay Science 8, 187–192.

EN 772-7, 1998. Methods of tests for masonry units: Part 7. Determination of water absorption of clay masonry damp proof course unit by boiling water. Brussels, 5 pp.

EN ISO 12570, 2000. Hygrothermal performance of building materials and products—Determination of moisture content by drying at elevated temperature. Brussels. 11 pp.

Esbert, R.M., Ordaz, J., Alonso, F.J., Montoto, M., González Limón, T., Álvarez de Buergo Ballester, M., 1997. Manual de diagnosis y tratamiento de materiales pétreos y cerámicos. Collegi d'Apparelladors i Arquitectes Tècnics de Barcelona, Barcelona, pp. 89–106. Chap. 7.

Freestone, I.C., Middleton, A.P., 1987. Mineralogical applications of the analytical SEM in archaeology. Mineralogical Magazine 51, 21–31.

González García, F., Romero Acosta, V., García Ramos, G., González Rodríguez, M., 1990. Firing transformations of mixtures of clays containing illite, kaolinite and calcium carbonate used by ornamental tile industries. Applied Clay Science 5, 361–375.

GOST 7025-91, 1991. Ceramics and calcium silicate bricks and stones. Methods for water absorption and density determination and frost resistance control. Moscow. 11 pp.

Guydader, J., Denis, A., 1986. Propagation des ondes dans les roches anisotropes sous contrainte évaluation de la qualité des schistes ardoisiers. Bulletin Engineering Geology 33, 49–55.

Hansen, W., Kung, J.H., 1988. Pore structure and frost durability of clay bricks. Materials and Structures 21, 443–447.

Jordán, M.M., Sanfeliu, T., de la Fuente, C., 2001. Firing transformations of Tertiary clays used in the manufacturing of ceramic tile bodies. Applied Clay Science 20, 87–95.

Klaarenbeek, F.W., 1961. The development of yellow colours in calcareous bricks. Transactions of the British Ceramic Society 60, 738–772.

Kondratjeva, S., Hodireva, V., 2000. Latvian Dolomites. State Geology Survey, Riga. 79 pp.

Kreimeyer, R., 1987. Some notes on firing color of clay bricks. Applied Clay Science 2, 175–183.

Kretz, R., 1983. Symbols for rock-forming minerals. The American Mineralogist 68, 277–279.

Kursh, V., Stinkule, A., 1997. Mineral Deposits of Latvia. University of Latvia, Riga, pp. 68–91.

Letsch, J., Noll, W., 1983. Phasenbildung in einigen keramischen Teilsystemen bei 600–1000 °C in Abhangigkeit von Sauerstoffugazitat. Ceramic Forum International Beriete der Deutschen Keramischen Gesellschaft, 60. Heft 7.

Maage, M., 1980. Frost resistance and pore size distribution in bricks. Materials and Structures 17, 345–350.

Maniatis, Y., Simopoulos, A., Kostikas, A., 1981. Moessbauer study of the effect of calcium content in iron oxide transformations in fired clays. Journal of the American Ceramic Society 64-5, 263–269.

Manning, D.A.C., 1995. Introduction to Industrial Minerals. Chapman & Hall, London, pp. 159–184. Chap. 8.

Martín Ramos, J.D., 1990. Programa de control y análisis del difractómetro de rayos X. Dep. Leg. M-11719.

NORMAL 7/81, 1981. Assorbimento dell'acqua per immersione totale. Capacità di imbibizione. CNR-ICR, Roma. 5 pp.

NORMAL 29/88, 1988. Misura dell'indice di asciugamento (drying index). CNR-ICR, Roma. 9 pp.

Orts, M.J., Escardino, A., Amorós, J.L., Negre, F., 1993. Microstructural changes during firing of stoneware floor tiles. Applied Clay Science 8, 193–205.

Peters, T., Iberg, R., 1978. Mineralogical changes during firing of calcium-rich brick clays. Ceramic Bulletin 57 (5), 503–509.

Reimann, C., Siewers, U., Tarvainen, T., Bityukova, L., Eriksson, J., Gilucis, A., Gregorauskiene, V., Lukashev, V., Matinian, N.N., Pasieczna, A., 2000. Baltic soil survey: total concentrations of major and selected trace elements in arable soils from 10 countries around the Baltic Sea. The Science of the Total Environment 257, 155–170.

Rodríguez Gallego, M., Martín Pozas, J.M., Martín Vivaldi, J.L., 1968. Análisis cuantitativo de filosilicatos de la arcilla por difracción de rayos X: influencia de las sustituciones isomórficas y cristalinidad. Anuario de la Real Sociedad Española de Física y Química 65, 25–29.

Rodríguez Navarro, C., Cultrone, G., Sánchez Navas, A., Sebastián, E., 2003. TEM study of mullite growth after muscovite breakdown. The American Mineralogist 88, 713–724.

Singer, F., Singer, S.S., 1963. Industrial Ceramics, vol. 1. Chapman & Hall, London, pp. 200–274. Spanish version, Chap. 2.

Svinka, R., Svinka, V., 1997. Chemistry and Technology of Silicate Materials. University of Latvia, Riga, pp. 20–22.

Tite, M.S., Maniatis, Y., 1975. Examination of ancient pottery using the scanning electron microscope. Nature 257, 122–123.

Veniale, F., 1990. Modern techniques of analysis applied to ancient ceramics. Advanced Workshop "Analytical Methodologies for the Investigation of Damaged Stones", Pavia (Italy). Department of Earth Sciences, University of Pavia, Italy, 45 pp.